Design and Implementation of Vehicle Management System

IOP Conf. Series: Materials Science and Engineering **398** (2018) 012014 doi:10.1088/1757-899X/398/1/012014

Modal Analysis of a Compressor Disk

G Liu[1], W Zhang[2] and A Xi[3]

[1] College of Mechanical Engineering, Beijing University of Technology, Beijing, 100124, PR China
[2] College of Mechanical Engineering, Beijing University of Technology, Beijing, 100124, PR China
[3] College of Mechanical Engineering, Beijing University of Technology, Beijing, 100124, PR China

liugen1991@hotmail.com

Abstract. The compressor disk is one of the key parts of the aeroengine. Its structure and strength play an important role in the reliability of the compressor. Most of the damage are caused by resonance stress. At the same time, the dynamic design and analysis of the key components are required because of the rotating state. When the compressor disk is in normal operation, the disk rotates around the rotating shaft in a large scale. Centrifugal inertia force will affect the deformation of the structure, and induce a certain change of natural frequency when compared to the static condition, which has increased complexity to modelling and numerical calculation. In this paper, the effect of dynamic stiffening on the vibration characteristics of disc is studied. In order to derive the equations of motion, Hamilton's principle is used, and the boundary conditions are obtained at the same time. We studied the natural frequency of the isotropic plate and laminate plate by Ritz method. Using the popular finite element analysis software ANSYS, we carry on simulation computation of vibration modes on a certain type of compressor in the working process. Besides, by investigation of the influence of structure parameter and rotating speed on the forward travelling wave and back travelling wave, we studied the critical speed of the compressor disk, which is essential in the rotator.

1. Introduction

Rotating structure, especially high speed rotating structure, is vulnerable under external disturbance and strong vibration. Sometimes a very small external perturbation would induce structural fracture, resulting in a serious accident. In recent years, many accidents have occurred in domestic and foreign aviation engines due to excessive vibration caused by the vibration of the disk fatigue damage. Therefore, research on transverse vibration characteristics of rotating circular plate under high speed has very important engineering value.

A perturbation technique had been used by Park et al. [1] to investigate the free vibration behaviour of rotating disks, and by Baddour and Zu [2] to investigate the nonlinear dynamic behaviour of rotating disks. The study of transverse vibration behaviour of spinning circular disks having one of the various models, such as rectangular, cylindrical or polar, has also been carried out [3-4].

Powmya et al. [5] presented solutions, which were based on principle of collocating the equations of motion at Chebyshev zeroes for the free vibration analysis of laminated plate. Hashemi et al. [6] dealt with the free vibration behavior of laminated transversely isotropic circular plates with

axisymmetric rigid core attached to the center. Sujata et al. [7] showed that the fatigue crack of dimension as measured on the fracture surface is unstable, and it would lead to instantaneous fracture of the disk under the prevailing engine operating conditions. Debabrata et al. [8] studied the effects of the individual loadings and their combination on the free vibration dynamic behavior. Zhou [9] used the structural module of finite element of ANSYS to calculate the stress, deformation, natural frequency and mode shapes of gas compressor disc. The results show that the stress concentration occurred on balance hole.

It is evident from the literature review that research on large amplitude dynamic analysis of high rotating speed disc is scarce. At the same time, research on rotating disk of variable structure parameters is not available in the literature in spite of the tremendous potential in industrial applications. In this paper, the effect of dynamic stiffening on the vibration characteristics of disc is studied.

2. The modeling of compressor disk

2.1. Potential energy

The dynamic behaviour of a rotating annular disk having inner radius r_1 and outer radius r_2, rigidly mounted on a shaft, is investigated. The disk is considered to be flexible while the shaft is taken as a rigid body, as shown in Figure 1.

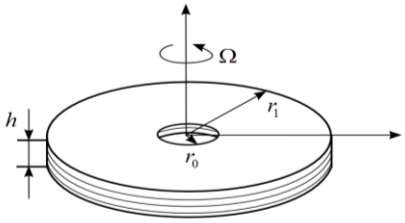

Figure 1. Schematic diagram of rotating disk

Also, the disk material is assumed to be isotropic and homogeneous and to follow linear elastic material behaviour.

In thin plate theory, it is usually assumed that the linear filaments of the plate initially perpendicular to the middle surface remain straight and perpendicular and do not contract or extend. This assumption leads to a relationship between the displacement of an arbitrary point and the displacements of the middle surface. They are given by,

$$u_r(\mathrm{r},\theta,\mathrm{z},\mathrm{t}) = u\left(r,\theta,t\right) + z\varphi_1\left(r.\theta,t\right) \tag{1a}$$

$$u_\theta(\mathrm{r},\theta,\mathrm{z},\mathrm{t}) = v\left(r,\theta,t\right) + z\varphi_2\left(r,\theta,t\right) \tag{1b}$$

$$u_z(\mathrm{r},\theta,\mathrm{z},\mathrm{t}) = w(r,\theta,t) \tag{1c}$$

Where u_r, u_θ, u_z denote the displacements of any point on the middle surface and φ_1,φ_2 are the rotations of the normal to the midplane about h, r axes, respectively.

The disk thickness is considered to be small compared to its outer radius in order to have the plane stress assumption for the present formulation valid and in order to neglect the effect of shear deformation and rotary inertia. When the transverse shear effects are neglected,

$$\varphi_1(\mathrm{r},\theta,\mathrm{t}) = -\frac{\partial w}{\partial r}, \varphi_2\left(r,\theta,t\right) = -\frac{\partial w}{r\partial\theta} \tag{2}$$

The von-Karman plate theory can be shown to lead to the following nonlinear stain-displacement expressions

$$\boldsymbol{\varepsilon}=\begin{Bmatrix}\varepsilon_r\\ \varepsilon_\theta\\ \varepsilon_{r\theta}\end{Bmatrix}=\begin{Bmatrix}\dfrac{\partial u_r}{\partial r}\\ \dfrac{u_r}{r}+\dfrac{1}{r}\dfrac{\partial u_\theta}{\partial \theta}\\ \dfrac{1}{2r}\left(\dfrac{\partial \mathrm{u_r}}{\partial \theta}-\mathrm{u}_\theta+\mathrm{r}\dfrac{\partial \mathrm{u}_\theta}{\partial \mathrm{r}}\right)\end{Bmatrix}+\begin{Bmatrix}\dfrac{1}{2}\left(\dfrac{\partial \mathrm{u_z}}{\partial \mathrm{r}}\right)^2\\ \dfrac{1}{2\mathrm{r}^2}\left(\dfrac{\partial \mathrm{u_z}}{\partial \theta}\right)^2\\ \dfrac{1}{2r}\dfrac{\partial \mathrm{u_z}}{\partial \mathrm{r}}\dfrac{\partial \mathrm{u_z}}{\partial \theta}\end{Bmatrix} \tag{3}$$

Substitute equations (1a-1c) to (3), we can obtain

$$\boldsymbol{\varepsilon}=\boldsymbol{\varepsilon_0}+\boldsymbol{\varepsilon_1}=\begin{Bmatrix}\dfrac{\partial u}{\partial r}+\dfrac{1}{2}\left(\dfrac{\partial w}{\partial \mathrm{r}}\right)^2\\ \dfrac{u}{r}+\dfrac{1}{r}\dfrac{\partial v}{\partial \theta}+\dfrac{1}{2\mathrm{r}^2}\left(\dfrac{\partial \mathrm{w}}{\partial \theta}\right)^2\\ \dfrac{1}{r}\left[\dfrac{\partial \mathrm{u}}{\partial \theta}-\mathrm{u}+\mathrm{r}\dfrac{\partial \mathrm{v}}{\partial \mathrm{r}}+\dfrac{\partial \mathrm{w}}{\partial \mathrm{r}}\dfrac{\partial \mathrm{w}}{\partial \theta}\right]\end{Bmatrix}+z\begin{Bmatrix}-\dfrac{\partial^2 w}{\partial r^2}\\ -\dfrac{\partial^2 w}{r^2\partial \theta^2}-\dfrac{\partial \mathrm{w}}{r\partial \mathrm{r}}\\ -2\dfrac{\partial \mathrm{w}}{\partial \mathrm{r}}\dfrac{\partial \mathrm{w}}{r\partial \theta}+\dfrac{\partial \mathrm{w}}{r^2\partial \theta}\end{Bmatrix} \tag{4}$$

Where $\boldsymbol{\varepsilon_0},\boldsymbol{\varepsilon_1}$ are linear and nonlinear strain vectors

According to the shear deformation theory, the constitutive equations for the *kth* layer of a polar orthotropic laminated plate can be written in the following form in polar co-ordinates

$$\begin{Bmatrix}\sigma_\mathrm{r}\\ \sigma_\theta\\ \sigma_{\mathrm{r}\theta}\end{Bmatrix}=\begin{bmatrix}\bar{Q}_{11} & \bar{Q}_{12} & 0\\ \bar{Q}_{21} & \bar{Q}_{22} & 0\\ 0 & 0 & \bar{Q}_{66}\end{bmatrix}\begin{Bmatrix}\varepsilon_\mathrm{r}\\ \varepsilon_\theta\\ \varepsilon_{\mathrm{r}\theta}\end{Bmatrix} \tag{5}$$

$$\begin{Bmatrix}\bar{Q}_{11}\\ \bar{Q}_{12}\\ \bar{Q}_{22}\\ \bar{Q}_{66}\end{Bmatrix}=\begin{bmatrix}C^4 & 2C^2S^2 & S^4 & 4C^2S^2\\ C^2S^2 & C^4+S^4 & C^2S^2 & -4C^2S^2\\ S^4 & 2C^2S^2 & C^4 & 4C^2S^2\\ C^2S^2 & -2C^2S^2 & C^2S^2 & (C^2-S^2)^2\end{bmatrix}\begin{Bmatrix}Q_{11}\\ Q_{12}\\ Q_{22}\\ Q_{66}\end{Bmatrix} \tag{6}$$

where $C=\cos\theta, S=\sin\theta$, $Q_{11,}Q_{12,}Q_{22,}Q_{66}$ are the elastic constants are expressed in terms of material constants in the plate co-ordinates as

$$Q_{11}=\frac{E_1}{1-\mu_{12}\mu_{21}}, Q_{12}=\mu_{12}\frac{E_1}{1-\mu_{12}\mu_{21}},\ Q_{22}=\frac{E_2}{1-\mu_{12}\mu_{21}}, Q_{66}=G_{12}=\frac{E}{2(1+\mu)}$$

where E is Young's modulus of elasticity , μ is Poisson's ratio.

The stress resultants acting on a laminate are obtained as,

$$U=\frac{1}{2}\iiint\left(\sigma_r\varepsilon_r+\sigma_\theta\varepsilon_\theta+\sigma_{r\theta}\varepsilon_{r\theta}\right)rdrd\theta dz \tag{7}$$

2.2. Kinetic energy

The original position of a particle is given by

$$\boldsymbol{r}_0=r\boldsymbol{e_r}+z\boldsymbol{e_z} \tag{8}$$

The deformed position of the same particle is given by

$$\boldsymbol{r}=\boldsymbol{r}_0+\boldsymbol{u}=(\mathrm{r}+\mathrm{u_r})\boldsymbol{e_r}+\mathrm{u}_\theta\boldsymbol{e_\theta}+(\mathrm{z}+\mathrm{u_z})\boldsymbol{e_z} \tag{9}$$

The velocity of this particle is obtained

$$\boldsymbol{v}=\frac{d\boldsymbol{r}}{d\boldsymbol{t}}=(\ \ldots\ )\boldsymbol{e_r}\ [\ \ldots\ ]\boldsymbol{e_\theta}\ \ldots\ \boldsymbol{e} \tag{10}$$

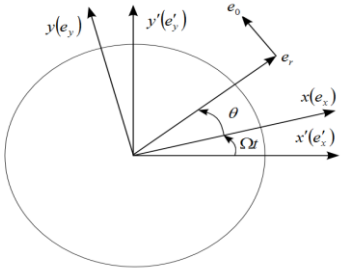

Figure2. Diagram of fixed coordinate system and dynamic coordinate system

According to the Figure 2, we can obtain

$$\frac{d\mathbf{e_r}}{dt}=\Omega\mathbf{e_\theta},\frac{d\mathbf{e_\theta}}{dt}=-\Omega\mathbf{e_r},\frac{d\mathbf{e_z}}{dt}=0 \tag{11}$$

Since the unit vectors are orthonormal, the square of the speed can be written as

$$\boldsymbol{v}\cdot\boldsymbol{v}=\left(i \right. \quad \left. \right] \tag{12}$$

$$T=\frac{1}{2}\rho\iiint\left(v\cdot v\right)rdrd\theta dz \tag{13}$$

In order to derive the equations of motion, Hamilton's principle is used

$$\begin{aligned}&\rho h\left[\frac{\partial^2u}{\partial t^2}-v\frac{\partial\Omega}{\partial t}-\Omega^2\left(r+u\right)-2\Omega\frac{\partial v}{\partial t}\right]=D_0\left[\frac{1+\mu}{2r}\frac{\partial^2v}{\partial r\partial\theta}+\frac{\partial^2u}{\partial r^2}-\frac{3-\gamma}{2r^2}\frac{\partial v}{\partial\theta}-\frac{1+\mu}{2r^3}\left(\frac{\partial w}{\partial\theta}\right)^2-\frac{u}{r^2}+\frac{\partial u}{r\partial r}\right]\\&+D_0\left[\frac{\partial w}{\partial r}\frac{\partial^2w}{\partial r^2}+\frac{1+\mu}{2r^2}\frac{\partial w}{\partial r}\frac{\partial^2w}{\partial r\partial\theta}\right]+G\frac{h}{r}\left[\frac{1}{r}\frac{\partial^2u}{\partial\theta^2}+\left(\frac{\partial w}{\partial r}\right)^2+\frac{1}{r}\frac{\partial w}{\partial r}\frac{\partial^2w}{\partial r\partial\theta}\right]\end{aligned} \tag{14}$$

$$\begin{aligned}&\rho h\left[\frac{\partial^2v}{\partial t^2}+\left(r+u\right)\frac{\partial\Omega}{\partial t}-\Omega^2v+2\Omega\frac{\partial u}{\partial t}\right]=D_0\left[\frac{1+\mu}{2r}\frac{\partial w}{\partial r}\frac{\partial^2w}{\partial r\partial\theta}+\frac{3-\mu}{2r^2}\frac{\partial u}{\partial\theta}+\frac{1+\mu}{2r}\frac{\partial^2u}{\partial r\partial\theta}+\frac{1}{r^2}\frac{\partial^2v}{\partial\theta^2}+\frac{1}{r^3}\frac{\partial w}{\partial\theta}\frac{\partial^2w}{\partial\theta^2}\right]\\&+\frac{Gh}{r}\left[r\frac{\partial^2v}{\partial r^2}+\frac{1}{r}\frac{\partial w}{\partial\theta}\frac{\partial w}{\partial r}+\frac{\partial v}{\partial r}-\frac{v}{r}+\frac{\partial w}{\partial\theta}\frac{\partial^2w}{\partial r^2}\right]\end{aligned} \tag{15}$$

$$\begin{aligned}&\rho h\left[\frac{\partial^2w}{\partial t^2}++\frac{h^2\Omega^2}{3}\nabla^2w-\frac{h^2\partial^2}{3\partial t^2}\nabla^2w\right]=D_0\left[-\frac{h^2}{3}\nabla^4w+\frac{3}{2r^4}\left(\frac{\partial w}{\partial\theta}\right)^2\frac{\partial^2w}{\partial\theta^2}+\frac{1}{r^3}\frac{\partial^2v}{\partial\theta^2}\frac{\partial w}{\partial\theta}-\frac{1}{2r^3}\left(\frac{\partial w}{\partial\theta}\right)^2\frac{\partial w}{\partial r}\right]\\&+D_0\frac{1+\mu}{2}r\frac{\partial w}{\partial\theta}\frac{\partial u}{\partial\theta}+D_0\frac{\partial w}{\partial\theta}\left[+\frac{1+\mu}{2}r^2\frac{\partial^2u}{\partial r\partial\theta}+\frac{1-\mu}{2}rv\right]+D_0\frac{\partial w}{\partial\theta}\left[\frac{r^2}{2}\frac{\partial w}{\partial\theta}\frac{\partial^2w}{\partial r^2}+r^2\frac{\partial w}{\partial r}\frac{\partial^2w}{\partial r\partial\theta}+\frac{1-\mu}{2}r^3\frac{\partial^2v}{\partial r^2}-\frac{1-\mu}{2}r^2\frac{\partial v}{\partial r}\right]\\&+\frac{1}{r^4}\frac{\partial w}{\partial r}\left[r^2\frac{\partial w}{\partial\theta}\frac{\partial^2w}{\partial r\partial\theta}+(1+\mu)\mathrm{r}^3\frac{\partial u}{\partial r}+\frac{1+\mu}{2}r^3\frac{\partial^2v}{\partial r\partial\theta}\right]+\frac{1}{r^4}\frac{\partial w}{\partial r}\left[\frac{1-\mu}{2}r^2\frac{\partial^2u}{\partial\theta^2}+\frac{r^3}{2}(\frac{\partial w}{\partial r})^2+\frac{r^2}{2}\frac{\partial w}{\partial r}\frac{\partial^2w}{\partial\theta^2}+r^4\frac{\partial^2u}{\partial r^2}+\frac{3r^4}{2}\frac{\partial w}{\partial r}\frac{\partial^2w}{\partial r^2}\right]\\&-\frac{1-\mu}{2}r^2\frac{\partial v}{\partial\theta}\frac{1}{r^4}\frac{\partial w}{\partial r}+\frac{1}{r^4}\frac{\partial^2w}{\partial\theta}\left[vr\frac{\partial u}{\partial r}+r(\mathrm{u}+\frac{\partial v}{\partial\theta})\right]+\frac{\partial^2w}{\partial r^2}\left[\frac{\partial u}{\partial r}+\frac{v}{r}(\mathrm{u}+\frac{\partial v}{\partial\theta})\right]+\frac{1-\mu}{r^2}\frac{\partial^2w}{\partial r\partial\theta}\left[\frac{\partial u}{\partial\theta}-v+r\frac{\partial v}{\partial r}\right]\end{aligned} \tag{16}$$

Where

$$D_0=\frac{Eh}{\left(1-\mu^2\right)},\nabla^2=\frac{\partial}{\partial r^2}+\frac{1}{r}\frac{\partial}{\partial r}+\frac{1}{r^2}\frac{\partial^2}{\partial\theta^2}$$

The boundary term obtained is given below

$$\frac{\partial}{\partial r}\left(\nabla^2w\right)-\frac{1-\mu}{r^2}\frac{\partial^2}{\partial\theta^2}\left(\frac{\partial w}{\partial r}-\frac{w}{r}\right)=0 \qquad \frac{\partial^2w}{\partial r^2}+\frac{\gamma}{r}\frac{\partial w}{\partial r}+\frac{\gamma}{r^2}\frac{\partial^2w}{\partial\theta^2}=0$$

$$\frac{\partial u}{\partial r}+\frac{1}{2}\left(\frac{\partial w}{\partial r}\right)^2+\frac{\mu}{r}\left(\frac{\partial v}{\partial \theta}+u\right)+\frac{\mu}{2}\left(\frac{\partial w}{r\partial \theta}\right)^2=0 \qquad \frac{\partial u}{r\partial \theta}+\frac{\partial v}{\partial r}-\frac{v}{r}+\frac{1}{v}\frac{\partial^2 w}{\partial r\partial \theta}=0$$

Dynamic characteristics of transverse vibration of rotating circular plate can be described by the "wave theory" and "critical speed" theory. The vibration of a section is composed of two traveling waves in the opposite direction: forward traveling wave and backward traveling wave,

$$f_f=f_d+n\Omega \tag{17}$$

$$f_b=f_d-n\Omega \tag{18}$$

The n is the number of nodal radius. Apparently, when n=0, the frequency of forward travelling wave and backward travelling wave are the same. While when n⩾1, the frequency of forward traveling wave is bigger than backward traveling wave. When fb = 0, which means Ω= fb/n is the critical speed.

When a thin circular plate rotates at constant angular velocity, the equilibrium equation of the plate in the radial direction is expressed as

$$d\left(hr\sigma_r\right)/dr-h\sigma_\theta+h\rho r^2\Omega^2=0 \tag{19}$$

The radial and circumferential stress components in the equation are written as

$$\sigma_r=\frac{E}{1-\mu^2}\left(\mu\frac{u}{r}+\frac{du}{dr}\right),\sigma_\theta=\frac{E}{1-\mu^2}\left(\frac{u}{r}+\mu\frac{du}{dr}\right) \tag{20}$$

Substituting u and v into yields the equation

$$r^2\frac{d^2u}{dr^2}+r\frac{du}{dr}-u=\frac{1-\mu^2}{E}\rho r^3\Omega^2 \tag{21}$$

The general solution of equation (21) is obtained as

$$u=Ar+Br^{-1}-\frac{1-\mu^2}{8E}\rho r^3\Omega^2 \tag{22}$$

Combining the boundary conditions, the unknown coefficients can be obtained as follows

$$A=\frac{\left(1-\mu^2\right)\rho\Omega^2}{8E\left[r_0^{\,2}\left(1+\mu\right)+r_1^{\,2}\left(1-\mu\right)\right]}\left[r_0^{\,4}\left(3+\mu\right)+r_1^{\,4}\left(1-\mu\right)\right] \tag{23}$$

$$B=-\frac{\left(1-\mu^2\right)\rho\Omega^2 r_0^{\,2}r_1^{\,2}}{8E\left[r_0^{\,2}\left(1+\mu\right)+r_1^{\,2}\left(1-\mu\right)\right]}\left[r_0^{\,2}\left(3+\mu\right)-r_1^{\,2}\left(1+\mu\right)\right] \tag{24}$$

3. Solution

To set up the eigen value problem for determination of free
vibration frequencies and the corresponding mode shapes in the present work, we can write the displacements in the form as follows

$$u\left(r,\theta,t\right)=\sum_{m=0}^{M}C_{rmn}V_{rmn}e^{i\left(n\theta+\lambda t\right)} \tag{25a}$$

$$v\left(r,\theta,t\right)=\sum_{m=0}^{M}C_{\theta mn}V_{\theta mn}e^{i\left(\frac{\pi}{2}n\theta+\lambda t\right)} \tag{25b}$$

$$w\left(r,\theta,t\right)=\sum_{m=0}^{M}C_{wmn}V_{wmn}e^{i\left(n\theta+\lambda t\right)} \tag{25c}$$

Where m, n are the number of the node cycle and the number of node diameter of the disk mode, M is the truncation order.

By substituting equations (7) and (13) into the Lagrange function, neglecting nonlinear terms

$$L=T_{\max}-U_{\max} \tag{26}$$

According to the Ritz method,

$$\frac{\partial L}{\partial C_{rmn}}=0,\frac{\partial L}{\partial C_{\theta mn}}=0,\frac{\partial L}{\partial C_{wmn}}=0 \tag{27}$$

The following frequency equations are derived

$$\left(K-\lambda^2 M\right)S=0 \tag{28}$$

Where K is the stiffness matrix, M is the mass matrix and S is the coefficients matrix, which can be written

$$S=\left\{C_{r01}...C_{r1n}...C_{rmn},C_{\theta 01}...C_{\theta 1n}...C_{\theta mn},C_{w01}...C_{w1n}...C_{wmn}\right\}$$

4. Numerical results and discussions

4.1. Modal analysis of the disk

The example model in this study is from the first-stage disk of the low-compressor in some type of aeroengine. The model parameters of isotropic plate are listed in Table 1.

Table 1. Parameters of isotropic plate

Structural parameters	Symbols	Values
Inner radius	r_0	30mm
Outer radius	r_1	90mm
Thickness	h	8mm
Density	ρ	7840kg/m^3
Young's modulus	E	210Gpa
Poisson's ratio	μ	0.3

Laminate plate parameters are: the number of layer k=8, the orientation is [0/45/-45/90], Ex=25x106N/m2, Ey=1x106N/m2, Gxy= Gxz =0.5x106N/m2, Gyz =0.2x106N/m2. The truncation order M=5, which can lead to good convergence.

The natural frequency and corresponding nodal diameter and nodal cycle are listed in Table 2.

Table 2. The natural frequency of a static and rotating disk

Mode (m, n)		**Ω**=0		**Ω**=12000r/min	
		isotropic	laminate	isotropic	laminate
(0.0)	FTW	919.80.	919.10	943.74	942.10
	BTW	919.80	919.10	943.74	942.10
(0.1)	FTW	954.27	953.96	967.21	967.10
	BTW	954.27	953.96	961.10	959.32
(0.2)	FTW	1107.81	1009.27	1121.43	1110.21
	BTW	1107.81	1009.27	1119.27	1109.10
(0.3)	FTW	1817.32	1815.31	1991.30	1971.24
	BTW	1817.32	1815.31	1984.32	1965.31
(0.4)	FTW	2183.81	2181.23	2278.43	2241.32
	BTW	2183.81	2181.23	2213.74	2201.78
(1.0)	FTW	2651.73	2649.54	2741.24	2710.37
	BTW	2651.73	2649.54	2720.34	3694.38
(1.1)	FTW	2783.49	2781.78	2841.32	2819.42
	BTW	2783.49	2781.78	2810.17	2801.38

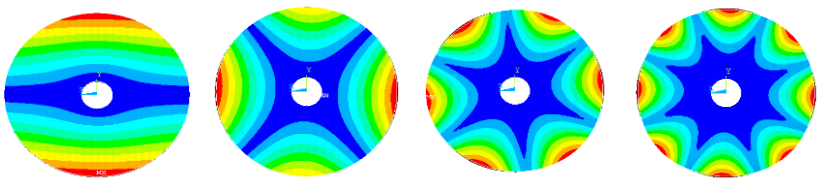

Mode (0, 1) Mode (0, 2) Mode (0, 3) Mode (0, 4)

Figure 3. Modal analysis of a compressor disk with pre-stress

From the Table 2, we can find that the dynamic frequency of the disc is larger than that of the static frequency due to the stress stiffening effect generated by the rotation. Besides, it is not difficult to find that with the increase of the node diameter, the amplitude of the dynamic frequency increases, and the amplitude is enlarged for the same node diameter.

4.2. The influence of structure parameter on natural frequency of the disk

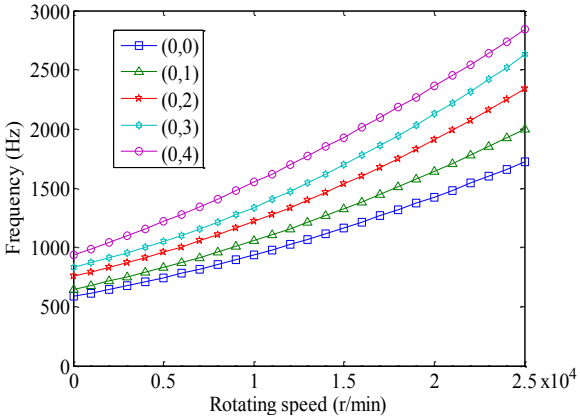

Figure 4

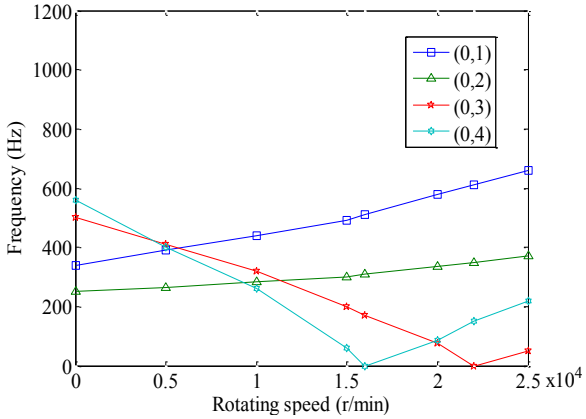

Figure 5

Figure 4. The natural frequency of isotropic plate with rotating speed (radius ratio=3, Backward travelling wave)

Figure 5. The natural frequency of isotropic plate various rotating speed (radius ratio=3, Forward travelling wave)

Since the critical speed is the angular velocity when the back traveling wave frequency is zero, the critical speed is the intersection of the back traveling wave frequency and the horizontal axis.

From the above two figures, the forward traveling wave frequency increases with the rotating speed increases, the back traveling wave frequency reduces with the rotating speed increases. Note that the critical speed of n=3 is greater than that of n=4.

There is non-intersection point of the back traveling wave and the horizontal axis when the number of node is 1 and 2, that is, there exists no critical speed. And for other higher-order modes, their vibration frequency increases at first with the increase of rotation speed and then decreases to zero, then the frequency is further increasing. That is to say, for laminated circular plate and single plate, there is also exit dynamic buckling phenomenon and has dynamic buckling critical speed.

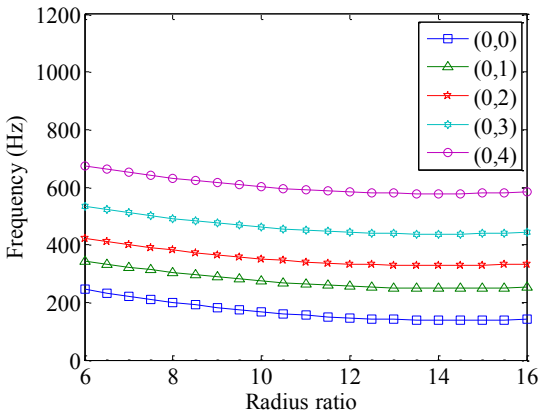

Figure 6

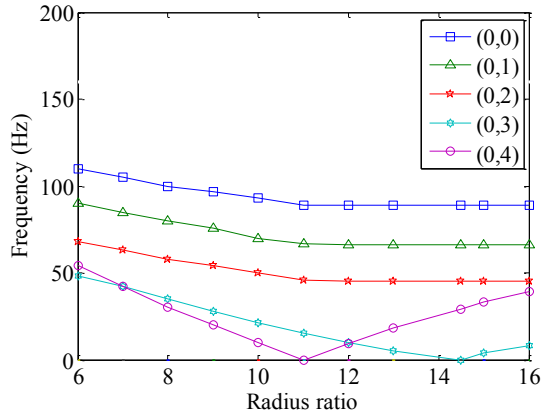

Figure 7

Figure 6. The natural frequency of laminate plate with various radius ratio (Ω=1200r/min, Forward travelling wave)

Figure 7. The natural frequency of laminate plate with various radius ratio (Ω=1200r/min, Backward travelling wave)

From the above two figures, we can obtain that when the radius ratio is over 10, the curve is relatively flat, which demonstrate the influence of radius ratio on the modal frequency of the front traveling wave is more and more small with the increase of the radius ratio. While the change trend of vibration frequency of back traveling wave is that with increase of the radius ratio, the frequency decreases to zero first and then increases. The reason could be due to that the increase of the radius ratio decreases the total bending stiffness of laminated circular plate, then makes the vibration frequency decrease.

4.3. Critical speed of the disk

The critical speed of dynamic instability is the most concerned parameter, which determines whether the whole vibration system is safe or not. Using the research of the influence of geometric parameter to circular plate, we could optimize the design and improve the system critical speed, in turn made the rotating circular plate work more stable. Here, we discussed the critical speed of laminated circular plate with different radius ratio.

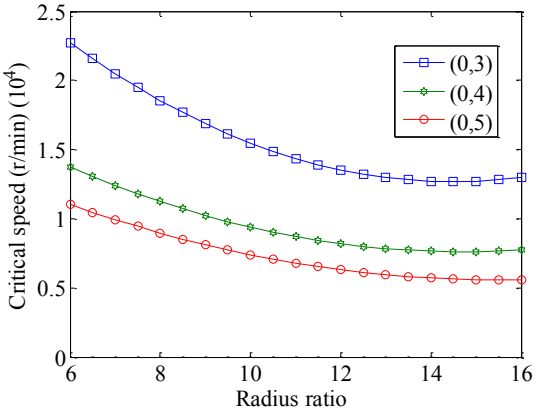

Figure 8. The critical speed of laminate plate with various radius ratio

Our results here show that for lower order modes n=0, n=1 and n=2, there does not appear the case that the back traveling wave vibration frequency is zero, that is, the three modes are stable. This figure also shows the change of the critical speed of 3 kinds of high order modes n=3, n=4 and n=5. From the graph, we can note that with the radius ratio increases, critical speed of each mode decrease. This is due to that the increase of radius ratio reduces the bending stiffness of layer laminated circular plates, which make the natural frequency decrease, then decreases the critical speed.

5. Conclusions

This paper established dynamic equation of the rotating circle plate and got the corresponding boundary conditions. As the Lagrange method is a good solution to solve the forward and back travelling wave mode identification problem, the effect of geometric parameters on the critical speed of rotating laminated circular plate are discussed. Conclusions are drawn as follows,

(1) Composite materials and isotropic materials have different material properties, such as elastic modulus, density and so on, so their natural frequency characteristics are different. According to the results obtained in Figure 10, to improve the dynamic performance of the structure and reduce the plate deformation with high rotating speed, composite structures are more appropriate than isotropic structures in experiencing the same motion.

(2) By numerical calculation, we confirm that the rotating circular plate has traveling wave vibration characteristics, namely with the increasing of the speed, forward travelling wave vibration frequency increases, while back travelling wave vibration frequency decreases to zero and then increases, which indicate that the there is a dynamic instability critical speed of the compressor disk.

(3) We discuss in detail the effect of structural parameters of laminated circular plate on the critical speed. With increase of radius ratio of the laminated circular plate, the forward traveling wave vibration frequency and critical speed decreased.

References

[1] Park J S, Shen I Y, Ku C P R, 2003 *J. appl. mech-t. asme*, 70, pp. 299–310.
[2] Natalie Baddour, Jean W. Zu, 2007 *Appl math model*, 31, pp.54-77.
[3] S.H.Hashemi, S.Farhadi, S.Carra, 2009 Journal of Sound and Vibration, 323, pp.366–384.
[4] Khoshnood A and Jalali M A, 2008 *J sound vib,* 314, pp. 147–160.
[5] Powmya A and Narasimhan M C, 2015 *Internatioal Jounal Advanced Structure Engenieering*, 7.pp.129-141.
[6] Hosseini-Hashemi Sh and Rezaee V, 2012 *J sound vib*, 331, pp.5581–5596.
[7] Sujata M and Jagannathan N, 2013, *Journal of Failure Analysis and Prevention*, 13, pp.437–444.
[8] Debabrata Das, Prasanta Sahoo, and Kashinath Saha, 2012 *International Journal for Computational Methods in Engineering Science and Mechanics*, 13,pp.37–59..
[9] Zhou peng, Hu Yu-li, 2005 *Machinery Design and Manufacture*,06(2),pp.06.